

**(Sr, Mn)TiO<sub>3</sub>: A Magnetolectric Multiglass**

V. V. Shvartsman, S. Bedanta, P. Borisov, and W. Kleemann\*

*Angewandte Physik, Universität Duisburg-Essen, Lotharstrasse 1, 47048 Duisburg, Germany*

A. Tkach and P. M. Vilarinho

*Department of Ceramics and Glass Engineering, CICECO, University of Aveiro, 3810-193, Aveiro, Portugal*

(Received 8 February 2008; published 16 October 2008)

By close analogy with multiferroic materials with coexisting long-range electric and magnetic orders a “multiglass” scenario of two different glassy states is observed in Sr<sub>0.98</sub>Mn<sub>0.02</sub>TiO<sub>3</sub> ceramics. Sr-site substituted Mn<sup>2+</sup> ions are at the origin of both a polar and a spin glass with glass temperatures  $T_g \approx 38$  K and  $\leq 34$  K, respectively. The structural freezing triggers that of the spins, and both glassy systems show individual memory effects. Thanks to strong spin-phonon interaction within the incipient ferroelectric host crystal SrTiO<sub>3</sub>, large higher order magnetolectric coupling occurs between both glass systems.

DOI: [10.1103/PhysRevLett.101.165704](https://doi.org/10.1103/PhysRevLett.101.165704)

PACS numbers: 64.70.P-, 75.50.Lk, 77.22.-d, 77.84.Dy

Recent years have seen a growing research interest in materials exhibiting the linear magnetolectric (ME) effect [1,2]. It describes the cross-linking dependence of the magnetization and polarization on applied electric and magnetic fields, respectively. Since it promises to reach largest values in materials with both high electric and magnetic susceptibility [3], a most favorable situation might be realized in multiferroic materials, where two different ferroic states, e.g., ferroelectric and ferromagnetic, coexist [4]. However, the occurrence of linear magnetolectricity is very rare because of its high symmetry demands. For this reason it may even be absent in multiferroics as exemplified, e.g., by BiMnO<sub>3</sub> with  $T_C^{FM} = 100$  K [5] and  $T_C^{FE} = 440$  K [6], respectively. Only higher order magnetolectricity is predicted similarly as for systems without well-defined symmetry [7].

In this situation it seems meaningful to investigate the converse situation, namely, the ME coupling of disordered systems, e.g., given by glassy materials which have by definition neither electric nor magnetic periodic long-range order. In this Letter we show that the class of ME materials may, indeed, be extended to those undergoing transitions into glassy (or frozen metastable) states. These are well known to occur as a result of competing interactions and topological frustration, where the glass transition temperature  $T_g$  separates the ergodic high temperature regime,  $T > T_g$ , from the nonergodic low- $T$  one. At  $T < T_g$  true thermodynamic equilibrium can be reached only asymptotically. Structural and spin glass states at low  $T$  are established by cooperative random freezing of the orientational [8] and of the spin degrees of freedom, respectively [9]. Here we report on the simultaneous occurrence of a polar cluster glass and a magnetic spin glass state and on their mutual higher order ME coupling in (Sr<sub>1-x</sub>Mn<sub>x</sub>)TiO<sub>3</sub> (SMnT, for short) with  $x = 0.02$ .

SrTiO<sub>3</sub> is an incipient ferroelectric, whose polar instability is suppressed by quantum fluctuations, such that the system remains in the paraelectric state down to 0 K [10].

Polar order in STO may be induced by ionic substitutions as in (Sr<sub>1-x</sub>Ca<sub>x</sub>)TiO<sub>3</sub> [11]. In the related solid solution SMnT with  $x \leq 0.03$ , slim polarization vs electric-field hysteresis loops and a broad strongly frequency dependent peak of the dielectric permittivity are found [12]. The polar state in these compounds is due to off-center shifts of the Mn<sup>2+</sup> cations at the 12-fold coordinated A-cation Sr<sup>2+</sup> positions within the perovskite structure as depicted in Fig. 1(a) and evidenced by energy dispersive X-ray spectra [12] and by ESR techniques [13]. The off-center Mn<sup>2+</sup> cations are assumed to create dipoles, which induce polar clusters in the highly polarizable SrTiO<sub>3</sub> host lattice [14]. The situation resembles the related (nonmagnetic) system (K<sub>1-x</sub>Li<sub>x</sub>)TaO<sub>3</sub> (KLT) [8], which undergoes a transition into a generic glass state at  $T_g < 40$  K for  $x < 0.022$  [15]. In the case of SMnT [Fig. 1(a)] a six-state Potts glass referring to six discrete directions of the polar order parameter [16] is supposed to occur.

Ceramic samples SMnT with  $x = 0.02$  were prepared by a mixed oxide technology described elsewhere [12].

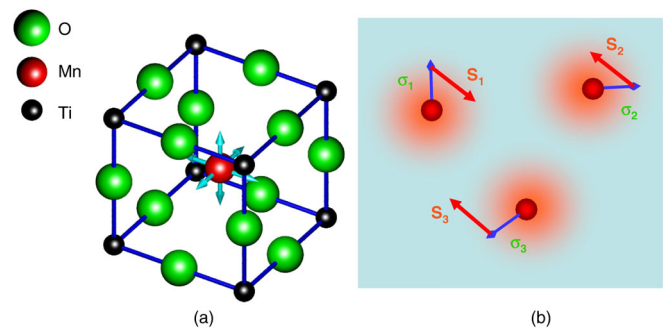


FIG. 1 (color online). (a) Displacement vectors of an off-center Mn<sup>2+</sup> ion in its cage of 12 surrounding oxygen ions of A-site doped SrTiO<sub>3</sub>. (b) Frustrated arrangement of three anti-ferromagnetically interacting Mn<sup>2+</sup> spins,  $S_j$ ,  $j = 1, 2$  and  $3$ , occupying frozen off-center positions  $\sigma_j$  of the structural glass backbone.

Figure 2(a) shows the temperature dependence of the real part of the dielectric permittivity  $\varepsilon'(T)$  recorded at frequencies  $10^{-1} \leq f < 10^6$  Hz. The position of the peak temperature  $T_m$  of  $\varepsilon'(T)$  is well described by a power law of the respective frequency,  $f(T_m) \propto (T_m/T_g^e - 1)^{z\nu}$  [Fig. 2(b)], which is a typical manifestation of glassy critical behavior [17,18]. Best fits of the data yield the electric glass temperature  $T_g^e = 38.3 \pm 0.3$  K (arrow), and the dynamical critical exponent,  $z\nu = 8.5 \pm 0.2$ , which compares well with that of spin glass systems [17].

An essential indicator of the suspected structural glass state is the memory effect, which arises after isothermally annealing below  $T_g^e$ . Figure 2(b) shows the ‘‘hole’’ burnt into  $\varepsilon'(T)$  after a wait time  $t_w \approx 10.5$  h at  $T_w = 32.5$  K (arrow). We find an indentation at the ‘‘annealing’’ temperature  $T_w$ ,  $\Delta\varepsilon' = \varepsilon'_{\text{wait}}(T_w) - \varepsilon'_{\text{ref}}(T_w) \approx -6$ . It resembles that observed on the structural glass  $\text{KTa}_{0.973}\text{Nb}_{0.027}\text{O}_3$  [19] and signifies the asymptotic approach to the glassy ground state at  $T_w$ , via a decrease of the susceptibility. Since the glassy ground state varies as a function of the temperature, the system is ‘‘rejuvenating’’ at  $T$  sufficiently far from  $T_w$  [17]. Hence, the burnt ‘‘hole’’ is localized around  $T_w$ , while a global decrease would be expected for an ordinarily relaxing metastable system. The small amplitude of the ‘‘hole’’ indicates that only a small fraction of dipoles is actually freezing. Indeed, it should be reminded that the structural glassy freezing of SMnT does not signify complete immobilization of all hopping  $\text{Mn}^{2+}$

ions [Fig. 1(a)]. Instead, just one percolating cluster freezes with  $\tau \rightarrow \infty$ , while ramifications and clusters of smaller size are still able to relax at  $f > 0$ . This is confirmed by the temperature dependence of the broad distribution of relaxation times as mimicked by  $\varepsilon''$  vs  $\log f$  [Fig. 2(c)]. Its low- $f$  tail gradually lifts upon cooling and attains a finite amplitude at  $f_{\text{min}} \rightarrow 0$  as  $T \rightarrow T_g^e$ . Similar relaxation spectra of  $\text{K}_{0.989}\text{Li}_{0.011}\text{TaO}_3$  [15] and of the spin glass manganese aluminosilicate [20] were taken as fingerprints of glass transitions.

Figure 3(a) shows the temperature dependences of the real and imaginary parts of the magnetic ac susceptibility,  $\chi' - i\chi''$ . Pronounced peaks with comparably weak polydispersivity [cf. Fig. 2(a)] are observed for frequencies  $0.1 \leq f \leq 10$  Hz slightly below  $T_g^e \approx 38$  K [inset to Fig. 3(a)]. Convergence of the  $\chi'$  vs  $T$  peaks occurs at  $T_g^m \leq 34$  K [see also Fig. 3(b)], which is about 1 order of magnitude larger than  $T_g^m$  observed on other manganese doped insulators like aluminosilicate [21]. Since the average distance between  $\text{Mn}^{2+}$  ions in SMnT ( $x = 0.02$ ),  $\langle d \rangle \approx 1.5$  nm, is too large as to warrant stability of the spin glass structure solely by frustrated superexchange, an amplification effect needs to be considered. By analogy with the antiferromagnetic quantum paraelectric  $\text{EuTiO}_3$  [7] we assume the applicability of the Hamiltonian

$$H^{me} = -\delta_{me} \sum_{(i,j)} \sum_{(k,l)} \mathbf{S}_i \mathbf{S}_j \boldsymbol{\sigma}_k \boldsymbol{\sigma}_l, \quad (1)$$

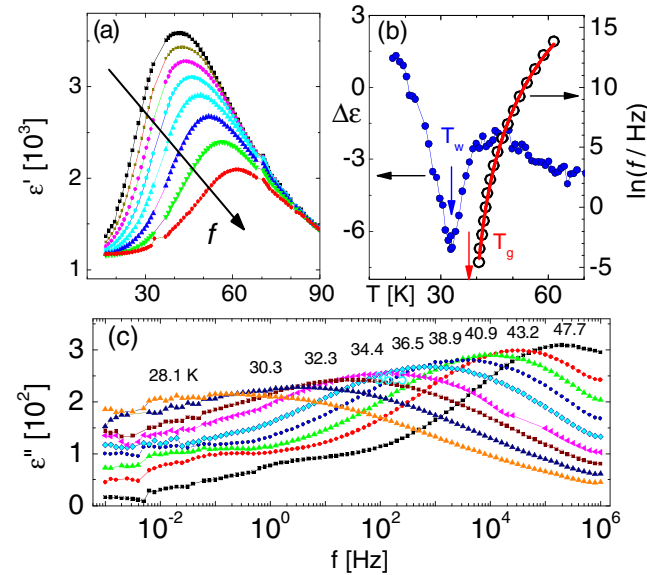


FIG. 2 (color online). (a)  $\varepsilon'(T)$  of  $\text{Sr}_{0.98}\text{Mn}_{0.02}\text{TiO}_3$  recorded at  $E_{\text{ac}} = 60$  V/m and frequencies  $f = 10^{-1}, 10^0, 10^1, 10^2, 10^3, 10^4, 10^5$ , and  $0.4 \times 10^6$  Hz. (b) Frequency dependence of the peak temperature ( $T_m$ ) of  $\varepsilon'(T)$  taken from (a) together with a critical power law fit (solid line) and difference curve  $\Delta\varepsilon' = \varepsilon'_{\text{wait}} - \varepsilon'_{\text{ref}}$  vs  $T$  obtained at  $f = 10$  Hz upon heating after ZFC from 110 K with and without waiting for 10.5 h at  $T_w = 32.5$  K, respectively. (c)  $\varepsilon''(f)$  of  $\text{Sr}_{0.98}\text{Mn}_{0.02}\text{TiO}_3$  recorded at frequencies  $10^{-3} \leq f \leq 10^6$  Hz.

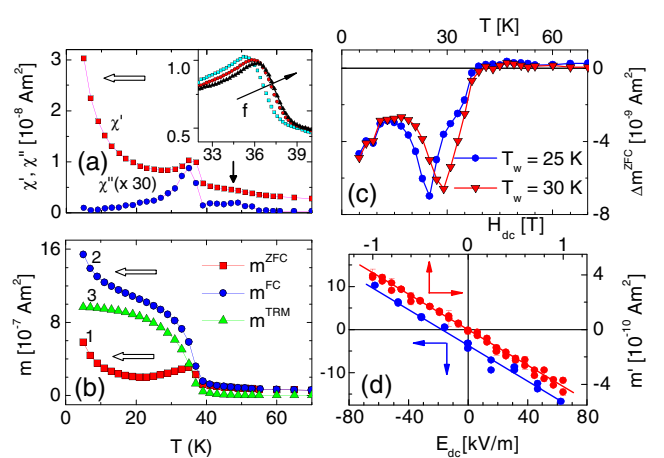


FIG. 3 (color online). (a) Temperature dependences of the real and imaginary parts,  $\chi'$  and  $\chi''$ , of the magnetic ac susceptibility of  $\text{Sr}_{0.98}\text{Mn}_{0.02}\text{TiO}_3$  measured at  $f = 1$  Hz with a field amplitude  $\mu_0 H_{\text{ac}} = 0.4$  mT (inset: expanded view of  $\chi'$  around  $T_g$  for frequencies  $10^{-1} \leq f \leq 10$  Hz). (b) Temperature dependences of  $m^{\text{ZFC}}$  (curve 1),  $m^{\text{FC}}$  (2), and  $m^{\text{TRM}}$  (3) measured in  $\mu_0 H = 10$  mT. (c) Difference curves of  $m^{\text{ZFC}}$  after ZFC from 110 to 5 K with and without intermittent stop of  $t_w = 10^4$  s at  $T_w = 25$  and 30 K. (d) Real part  $m'$  of the ME ac susceptibility measured at  $T = 10$  K and  $f = 1$  Hz in an ac electric field with amplitude  $E_{\text{ac}} = 62.5$  kV/m vs  $H_{\text{dc}}$  ( $-1 \leq \mu_0 H_{\text{dc}} \leq 1$  T; upper line) and vs  $E_{\text{dc}}$  ( $-62.5 \leq E_{\text{dc}} \leq 62.5$  kV/m under a bias field  $\mu_0 H_{\text{dc}} = 1$  T; lower line).

which describes the biquadratic coupling of spins  $\mathbf{S}_{i,j}$  and structural pseudospins  $\boldsymbol{\sigma}_{i,j}$  represented by unit vectors along  $\langle 100 \rangle$ , and has explained both the observed large spin-phonon coupling [7,22] and the magnetocapacitive effect in  $\text{EuTiO}_3$  [23]. The components of the pseudospins  $\boldsymbol{\sigma}_{i,j}$  mimic the off-center displacements of the  $A$  site dopant ions ( $\text{Mn}^{2+}$ ) being strongly coupled to the displacements of the  $B$  site ( $\text{Ti}^{4+}$ ) ions, which participate in the optic soft mode.  $\delta_{\text{me}}$  is an effective coupling constant. The displacement correlation functions couple to the  $S = 5/2$  Heisenberg spins  $\mathbf{S}_{i,j}$  of the  $3d^5$  configuration of the  $\text{Mn}^{2+}$  ions. Large effects are expected around  $T_g$ , where the structural pair-correlation functions  $\langle \boldsymbol{\sigma}_k \boldsymbol{\sigma}_l \rangle$  maximize, promote increased spin pair-correlation functions  $\langle \mathbf{S}_i \mathbf{S}_j \rangle$ , and give rise to weak anomalies of the magnetic susceptibility already above  $T_g$  [Fig. 3(a), vertical arrow]. Below  $T_g^e \approx 38$  K, the onset of a percolating network of frozen polar clusters probably triggers the freezing of the spin degrees of freedom. While above  $T_g^e$  freezing of the  $\text{Mn}^{2+}$  spins is suppressed by the hopping motion of the  $\text{Mn}^{2+}$  ions, those spins residing on the percolating polar glass cluster have a chance to achieve a well-defined collective state at  $T < T_g^e$ . Its glassy nature is provided by frustrated antiferromagnetic superexchange interaction via Mn-O-Mn chains similarly as in manganese aluminosilicate spin glasses [21]. Figure 1(b) shows a sketch of a possible local spin configuration at three sites of the frozen structural cluster.

Figure 3(b) shows the temperature dependence of the total magnetic moment  $m$  induced by  $\mu_0 H = 10$  mT upon field heating after zero-field cooling (ZFC) to 5 K ( $m^{\text{ZFC}}$ , curve 1), subsequently upon field cooling (FC) again to  $T = 5$  K ( $m^{\text{FC}}$ , curve 2), and finally as the thermoremanent magnetic moment upon heating in zero field ( $m^{\text{TRM}}$ , curve 3). Typical of spin glass behavior, irreversibility occurs below  $T_g^m \approx 34$  K together with a peak in  $m^{\text{ZFC}}(T)$ . In addition, the concave shape of  $m^{\text{TRM}}(T)$  around 40 K signifies the decay of metastable field-induced rather than of spontaneous magnetization.

It is noticed that Curie-type low- $T$  paramagnetic components,  $\Delta m \propto 1/T$ , occur in both  $m^{\text{ZFC}}$  and  $m^{\text{FC}}$ , similarly as in the magnetic susceptibility,  $\chi' \propto 1/T$  [Figs. 3(a) and 3(b), horizontal arrows]. This indicates that a sizable fraction of uncoupled spins remains paramagnetic down to lowest temperatures. Its fraction is estimated by approximating the low-field  $m^{\text{ZFC}}(T)$  curve in Fig. 3(b) by Curie's law,  $m^{\text{ZFC}} = (Nm_0^2/3k_B T)\mu_0 H$ , both at high and low temperatures [ $N$  = number of paramagnetic ions,  $k_B$  = Boltzmann's constant,  $m_0 \approx 5\mu_B \approx m(\text{Mn}^{2+})$  [24] calculated from the Curie constant at  $T > 250$  K and the total number of  $\text{Mn}^{2+}$  ions,  $N \approx 1.3 \times 10^{19}$ ]. A  $1/m^{\text{ZFC}}$  plot (not shown) distinguishes a flat slope between 250 and 300 K from a steeper one below 30 K. This manifests the condensation process into the spin glass phase. From Curie's law we estimate that about 60%–70% of the  $\text{Mn}^{2+}$  ions remain paramagnetic at low  $T$ . This complies with the idea that only those spins are subject to glassy

freezing, which reside on the rare percolating dipolar glass cluster, and underlines the close neighborhood of frozen dipoles and spins [Fig. 1(b)].

A crucial test of the spin glass phase is the memory effect similarly as verified in the polar glass [Fig. 2(b)]. Figure 3(c) shows the differences between  $m^{\text{ZFC}}$  data recorded with and without an intermittent stop,  $\Delta m^{\text{ZFC}}(T) = m_{\text{wait}}^{\text{ZFC}}(T) - m_{\text{ref}}^{\text{ZFC}}(T)$ , obtained after wait times  $t_w = 10^4$  s at  $T_w = 25$  and 30 K ( $< T_g^m$ ). Sharply defined “hole burning” dips occur exactly at the respective  $T_w$  similarly as in Fig. 2(b). They clearly evidence memory and rejuvenation of the spin system like in atomic and superspin glasses [17].

The proposed biquadratic coupling, Eq. (1), enters the free energy density expansion [25] together with additional possible ME coupling terms, while spontaneous polarization and magnetization and bilinear ME coupling (due to the lack of an appropriate crystalline symmetry [26]) are absent:

$$F(\mathbf{E}, \mathbf{H}) = F_0 - \frac{1}{2} \varepsilon_0 \varepsilon_{ij} E_i E_j - \frac{1}{2} \mu_0 \mu_{ij} H_i H_j - \frac{\gamma_{ijk}}{2} H_i E_j E_k - \frac{\beta_{ijk}}{2} E_i H_j H_k - \frac{\delta_{ijkl}}{2} E_i E_j H_k H_l \quad (2)$$

under Einstein summation. The electric-field-induced magnetization components of

$$\begin{aligned} \mu_0 M_i &= -\partial F / \partial H_i \\ &= \mu_0 \mu_{ij} H_j + \beta_{ijk} E_j H_k + \gamma_{ijk} / 2 E_j E_k \\ &\quad + \delta_{ijkl} H_j E_k E_l \end{aligned} \quad (3)$$

are measured using ME SQUID susceptometry [27]. It involves ac and dc electric and magnetic external fields,  $E = E_{\text{ac}} \cos \omega t + E_{\text{dc}}$  and  $H_{\text{dc}}$ , and records the first harmonic complex ac magnetic moment,  $m'(t) = (m' - im'') \cos \omega t$ , where

$$m' = (\beta E_{\text{ac}} H_{\text{dc}} + \gamma E_{\text{ac}} E_{\text{dc}} + 2\delta E_{\text{ac}} E_{\text{dc}} H_{\text{dc}})(V/\mu_0) \quad (4)$$

( $V$  = sample volume) and  $m'' \approx 0$  at the measurement frequency  $f = \omega/2\pi = 1$  Hz. The orientation averaged coupling constants,  $\beta$ ,  $\gamma$ , and  $\delta$  were measured after cooling the sample in zero external fields to  $T = 10$  K.

First, we established that  $\mu_0 H_{\text{dc}} = 0$  at arbitrary values of  $E_{\text{dc}}$  yields  $m' \equiv 0$  within errors. This means that both the bilinear and the quadratic ME responses are absent,  $\alpha = 0 = \gamma$ , as expected for systems without magnetic long-range order [28].

Second, we applied  $E_{\text{ac}} = 62.5$  KV/m and  $E_{\text{dc}} = 0$ , and cycled the magnetic field,  $|\mu_0 H_{\text{dc}}| \leq 1$  T [Fig. 3(d), upper line]. The slope of the emerging linear hysteresis-free cycle yields  $\beta = \mu_0 \Delta m' / V E_{\text{ac}} \Delta H_{\text{dc}} \approx -3.0 \times 10^{-19}$  s/A. The corresponding electric-field dependent “paramagnetoelec-

tricity" susceptibility,  $\Delta m'/\Delta H_{dc} \propto E_{ac}$ , is allowed whenever the paramagnetic ions are located at sites with broken inversion symmetry [29] and do not require magnetic long-range order [28]. However, since the linear dependence of  $\Delta m'/\Delta H_{dc}$  on  $E_{ac}$  requires global inversion asymmetry, we assume the occurrence of some net polarization  $P_r$ , either by self-poling on zero-field cooling or during the first poling cycle at 10 K. Being metastable throughout the polar glass state,  $P_r$  controls the bilinear coupling, until  $\beta \rightarrow 0$  as  $T \rightarrow T_g$  on heating (not shown). This complies with the structure of Fig. 1(a), which becomes centrosymmetric above  $T_g$ . Details have yet to be explored.

Third, we applied  $E_{ac} = 62.5$  kV/m and  $\mu_0 H_{dc} = 1$  T, and cycled an electric field,  $|E_{dc}| \leq 62.5$  kV/m [Fig. 3(d), lower line]. According to Eq. (4) it reveals  $\beta EH$  and  $\delta HE^2$  from the intercept at  $E_{dc} = 0$  and from the slope of  $m'$  vs  $E_{dc}$ , respectively. Consistently, the same  $\beta$  value emerges as from the slope of the upper curve, while the biquadratic coefficient—being quantified for the first time to the best of our knowledge—is  $\delta = \mu_0 \Delta m' / (2VH_{dc} E_{ac} \Delta E_{dc}) \approx -9.0 \times 10^{-24}$  sm/VA. The negative sign of  $\delta$  seems to corroborate double glassiness, whose free energy is enhanced in uniform external fields. The value of  $\delta$  allows to predict an  $E^2 H^2$ -based magnetocapacitive effect  $\Delta \varepsilon / \varepsilon' \approx -5 \times 10^{-4}$ , where  $\Delta \varepsilon = \delta H^2 / \varepsilon_0 \approx -0.65$  inserting  $\mu_0 H = 1$  T and  $\varepsilon'(T = 10 \text{ K}, f = 1 \text{ Hz}) \approx 1300$  [Fig. 2(a)]. Its magnitude is about 2.5% of that found for  $\text{EuTiO}_3$  at  $\mu_0 H = 1$  T and  $T = 4$  K,  $\Delta \varepsilon / \varepsilon' \approx 2 \times 10^{-2}$  [23], matching to the dilution in  $\text{SMnT}$ ,  $x_{\text{Mn}} = 0.02$ .

In conclusion, when replacing  $\text{Sr}^{2+}$  ions in  $\text{SrTiO}_3$  by a small amount of magnetic  $\text{Mn}^{2+}$  ions, two processes are activated at low temperatures. On one hand, the  $\text{Mn}^{2+}$  ions take the role of electric and elastic pseudospins and undergo a transition into a polar 6-state Potts glass [16]. On the other hand, the  $S = 5/2$  spins, being attached to the  $\text{Mn}^{2+}$  ions, couple via frustrated antiferromagnetic superexchange, reinforced by ME two-spin-pseudospin interaction. They freeze into a spin glass state after the polar degrees of freedom come to rest below  $T_g^e = 38$  K. Both glassy phases are independently evidenced by their specific memory effects. Dipolar and magnetic “holes” have never before been burned into one and the same system. Strong ME coupling via both the generic “magnetocapacitive”  $E^2 H^2$  and the probably spurious “paramagnetoelectric”  $EH^2$  effects manifests the importance of quantum fluctuations in  $\text{SrTiO}_3$ . It should be noticed that these coupling schemes would also be valid, if  $\text{SMnT}$  were in a non-equilibrium [18] instead of a generic dipole glass state. Corroborating experiments on oriented  $(\text{Sr}, \text{Mn})\text{TiO}_3$  single crystals are desirable, but up to now mere  $A$ -site substitution has not yet been achieved [30].

Financial support by the European Community within STREP NMP3-CT-2006-032616 (MULTICERAL) and the Network of Excellence FAME (Contract No. FP6-500159-1), by Deutsche Forschungsgemeinschaft via KL306/38-3 and SFB 491, and by DAAD via Acções Integradas Luso-

Alemãs is gratefully acknowledged.

\*Author to whom correspondence should be addressed.  
wolfgang.kleemann@uni-due.de

- [1] M. Fiebig, *J. Phys. D* **38**, R123 (2005).
- [2] W. Eerenstein, N. D. Mathur, and J. F. Scott, *Nature (London)* **442**, 759 (2006).
- [3] W. F. Brown, R. M. Hornreich, and S. Shtrikman, *Phys. Rev.* **168**, 574 (1968).
- [4] N. Hur *et al.*, *Nature (London)* **429**, 392 (2004).
- [5] C. H. Yang *et al.*, *Europhys. Lett.* **74**, 348 (2006).
- [6] T. Kimura *et al.*, *Phys. Rev. B* **67**, 180401(R) (2003).
- [7] C. J. Fennie and K. M. Rabe, *Phys. Rev. Lett.* **96**, 205505 (2006); **97**, 267602 (2006).
- [8] U. T. Höchli, K. Knorr, and A. Loidl, *Adv. Phys.* **39**, 405 (1990).
- [9] K. Binder and A. P. Young, *Rev. Mod. Phys.* **58**, 801 (1986).
- [10] K. A. Müller and H. Burkard, *Phys. Rev. B* **19**, 3593 (1979).
- [11] J. G. Bednorz and K. A. Müller, *Phys. Rev. Lett.* **52**, 2289 (1984).
- [12] A. Tkach, P. M. Vilarinho, and A. L. Kholkin, *Appl. Phys. Lett.* **86**, 172902 (2005); *Acta Mater.* **53**, 5061 (2005); **54**, 5385 (2006).
- [13] V. V. Laguta *et al.*, *Phys. Rev. B* **76**, 054104 (2007).
- [14] A. Tkach, P. M. Vilarinho, and A. L. Kholkin, *J. Appl. Phys.* **101**, 084110 (2007).
- [15] F. Wickenhöfer, W. Kleemann, and D. Rytz, *Ferroelectrics* **124**, 237 (1991).
- [16] F. Y. Wu, *Rev. Mod. Phys.* **54**, 235 (1982).
- [17] P. E. Jönsson, *Adv. Chem. Phys.* **128**, 191 (2004).
- [18] Although a fit to the traditional Vogel-Fulcher “law”  $f_m(T) = f_0 \exp(T_a/[T_{VF} - T])$  is only slightly worse than the dynamical critical slowing-down fit [Fig. 2(b)] with reasonable parameters  $f_0 = 4.74 \times 10^9$  Hz and  $T_a = 282$  K, it must be discarded because of its low  $T_{VF} = 30$  K, which is in contradiction with hole burning observed at  $T_w = 32.5$  K  $> T_{VF}$  [Fig. 2(b)].
- [19] P. Doussineau, T. de Lacerda-Aroso, and A. Levelut, *Europhys. Lett.* **46**, 401 (1999).
- [20] L. E. Wenger, in *Lecture Notes in Physics* (Springer-Verlag, Berlin, 1983), Vol. 192, p. 60.
- [21] F. S. Huang *et al.*, *J. Phys. C* **11**, L271 (1978).
- [22] H. Wu, Q. Jiang, and W. Z. Shen, *Phys. Rev. B* **69**, 014104 (2004).
- [23] T. Katsufuji and H. Takagi, *Phys. Rev. B* **64**, 054415 (2001).
- [24] Ch. Kittel, *Introduction to Solid State Physics* (Wiley, New York, 1966), 3rd ed., p. 509.
- [25] J.-P. Rivera, *Ferroelectrics* **161**, 165 (1994).
- [26] L. D. Landau and E. M. Lifshitz, *Electrodynamics of Continuous Media* (Pergamon, Oxford, 1960), p. 119.
- [27] P. Borisov, A. Hochstrat, V. V. Shvartsman, and W. Kleemann, *Rev. Sci. Instrum.* **78**, 106105 (2007).
- [28] H. Schmid, *Ferroelectrics* **161**, 1 (1994).
- [29] S. L. Hou and N. Bloembergen, *Phys. Rev.* **138**, A1218 (1965).
- [30] A. G. Badalyan *et al.*, *J. Phys. Conf. Ser.* **93**, 012012 (2007).